Structural and Electronic Properties of Pt13 Nanoclusters on Amorphous Silica Supports

ARTICLE *in* THE JOURNAL OF PHYSICAL CHEMISTRY C · FEBRUARY 2015

Impact Factor: 4.77 · DOI: 10.1021/jp5105104

THE JOURNAL OF PHYSICAL CHEMISTRY C

Article

pubs.acs.org/JPCC

Structural and Electronic Properties of Pt_{13} Nanoclusters on Amorphous Silica Supports

Christopher S. Ewing,[†,‡] Michael J. Hartmann,[§] Kaitlin R. Martin,[†] Allison M. Musto,[§] Surya J. Padinjarekutt,[§] Elliott M. Weiss,[†] Götz Veser,[†,‡,∥] Joseph J. McCarthy,[†] J. Karl Johnson,[†,∥] and Daniel S. Lambrecht*[,§]

[†]Department of Chemical and Petroleum Engineering, University of Pittsburgh, 3700 O'Hara Street, Pittsburgh, Pennsylvania 15206, United States

[‡]Mascaro Center for Sustainable Innovation, University of Pittsburgh, Pittsburgh, Pennsylvania 15261, United States

[§]Department of Chemistry, University of Pittsburgh, 219 Parkman Avenue, Pittsburgh, Pennsylvania 15206, United States

[∥]National Energy Technology Laboratory, Pittsburgh, Pennsylvania 15236, United States

Supporting Information

ABSTRACT: An accurate description of metal nanoparticle (NP)−support interactions is required for designing and optimizing NP catalytic systems because NP−support interactions may significantly impact NP stability and properties, such as catalytic activity. The ability to calculate NP interactions with *amorphous* supports, which are commonly used in industrial practice, is hampered because of a general lack of accurate atomically detailed model structures of amorphous surfaces. We have systematically studied relaxation processes of Pt_{13} NPs on amorphous silica using recently developed realistic model amorphous silica surfaces. We have modeled the NP relaxation process in multiple steps: hard-sphere interactions were first used to generate initial placement of NPs on amorphous surfaces, then Pt−silica bonds were allowed to form, and finally both the NP and substrate were relaxed with density functional theory calculations. We find that the amorphous silica surface significantly impacts the morphology and electronic structure of the Pt clusters. Both NP energetics and charge transfer from NP to the support depend linearly on the number of Pt−silica bonds. Moreover, we find that the number of Pt−silica bonds is determined by the silica silanol number, which is a function of the silica pretreatment temperature. We predict that catalyst stability and electronic charge can be tuned via the pretreatment temperature of the support materials. The extent of support effects suggests that experiments aiming to measure the intrinsic catalytic properties of very small NPs on amorphous supports will fail because the measurable catalytic properties will depend critically on metal−support interactions. The magnitude of support effects highlights the need for explicitly including amorphous supports in atomistic studies.

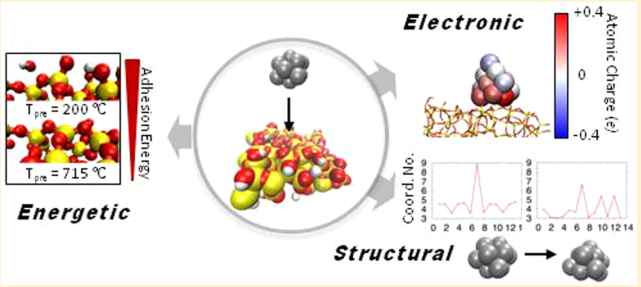

INTRODUCTION

Metal nanoparticles (NPs) have attracted considerable attention in the field of heterogeneous catalysis because of their large surface-to-volume ratios and low-coordinated active surface sites.[1−10] These NPs are typically immobilized on oxide supports, which can affect the activity and selectivity of the NPs by altering their morphology and electronic structure.[6−9,11,12] As pointed out by Norskov et al.,[13] there is a critical need for a fundamental atomic-scale understanding of catalyst−support interactions because they can dramatically impact the electronic properties of the supported NP. This information cannot be obtained from experiments alone,[14] and current modeling approaches almost always ignore the amorphous nature of the support.[6,9−11,15,16] Generating atomistic models of supported NPs on amorphous supports poses challenges not faced when using crystalline surfaces, because of the diversity of surface features and atomic surface roughness. The present work focuses on the development of a transferable methodology for studying the relaxation of catalytic nanoparticles on amorphous supports; we apply this methodology to investigate catalyst−support interactions between Pt and amorphous silica.

Amorphous silica is a widely used catalyst support because of its good thermal stability, tunable porosity, and highly tunable specific surface area.[1,12] Silica-supported Pt has shown promise for methane conversion[17] as well as low temperature oxidation of formaldehyde[1] and ethylene.[5] Although silica is relatively inert, it can be expected that its diversity of surface features will result in a wide range of metal−support interactions involving both physisorption and covalent Pt−O and Pt−Si bond formation at higher temperatures. A number of experimental

Received: October 19, 2014
Revised: December 19, 2014
Published: January 26, 2015

DOI: 10.1021/jp5105104
J. Phys. Chem. C 2015, 119, 2503−2512

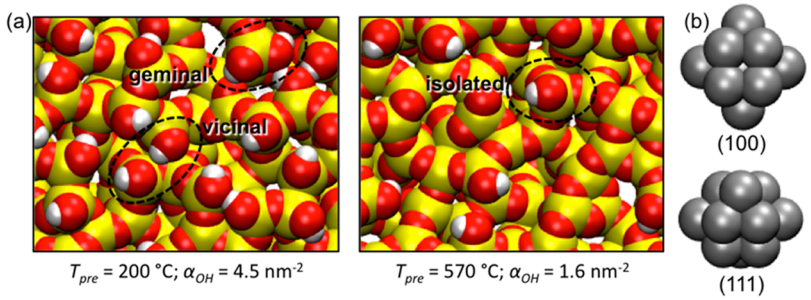

Figure 1. Top-down view of the structures used in this study. (a) Amorphous silica surfaces corresponding to pretreatment temperatures of 200 and 570 °C, based on analysis of experimental data by Zhuravlev.[21] Different types of silanol groups are illustrated. (b) Two initial orientations of cuboctahedral Pt_{13} corresponding to (100) (top) and (111) (bottom) surfaces facing downward upon adsorption. Images were rendered using VMD.[34]

studies have shown that the characteristics of the silica support, such as the concentration of surface silanols,[1] significantly affect Pt dispersion, catalytic activity, and thermal stability.[1,3,5,7,8,12,18,19] The atomistic origins of these effects, however, have remained elusive to date. Experiments have moved toward an atomistic understanding of these interactions by attempting to produce highly monodisperse supported NPs in order to probe the intrinsic catalytic activity as a function of size and shape.[20] However, given the importance of NP−support interactions, it is unclear whether (for amorphous supports) these interactions will induce a level of heterogeneity into the system that would make it impossible to reliably ascribe catalytic activity to a given NP size or shape. We aim to address these issues in this study for very small Pt NPs.

Silica has a large number of possible surface motifs that can be controlled in a straightforward way via the calcination temperature. Silanol groups (Si−OH) are typically formed on silica surfaces during synthesis and by exposure to water. Surface silanols can be classified as single, Si−OH, or geminal, $Si(OH)_2$. Each OH group can further be either vicinal, meaning that it is hydrogen bonded to a neighboring silanol, or free, meaning that it is not hydrogen bonded (see Figure 1). Silanol groups condense to form water vapor and siloxane bridge structures as the surface is heated, resulting in a reduction of the silanol number, α_{OH} (total surface silanol content, OH/nm^2).[21] Above ∼1200 °C the surface is exclusively terminated by siloxane bridges (Si−O−Si). It has been observed from experiments and modeling that α_{OH} and the silanol type (single, germinal, etc.) are strong functions of the thermal pretreatment (calcination) temperature, T_{pre}, of the silica support.[21,22] The interactions between NP and support depend on the silica surface groups present at the time of NP deposition, which in turn directly depend on T_{pre}. An atomistic understanding of metal−support interactions may thus allow for the optimization of stability and/or activity of silica supported NPs via the surface pretreatment conditions.

In this study we use density functional theory (DFT) calculations to investigate the impact of metal−support interactions on the morphology, electronic structure, and energetics of 13-atom Pt NPs supported on amorphous silica. Platinum clusters of this size (d = 0.7 nm) are small enough that metal−support interactions can significantly impact cluster morphology.[14] Crystalline surface models do not constitute realistic surrogates for amorphous silica because they exhibit only a small fraction of the configurations of surface features found on the real surface of amorphous silica. We therefore developed a procedure for generating supported Pt systems using accurate model structures of amorphous silica surfaces[22] to sample metal−support interactions for a large number of silica surface sites. Using this approach, we investigate the dependence of geometric and electronic properties of the supported Pt clusters on the variability of the amorphous silica surface. Our ultimate goal is to understand metal−support interactions and their role in catalysis for realistic model systems.

METHOD

Computational Details. For all DFT calculations we used the CP2K code, which employs a Quickstep[38] implementation of the DFT method using plane waves/pseudopotentials and localized Gaussian basis sets (see Supporting Information for details). Calculations used the revised PBE functional (revPBE)[39] and GTH pseudopotentials[40,41] in conjunction with short-range double-ζ basis sets with polarization functions (SR-DZVP).[42] All surface slabs were relaxed using CP2K treated as periodic in all directions with at least 20 Å of vacuum between slabs to eliminate interactions between the periodic images of the surface slabs. Validation of the planewave energy cutoff, basis sets, vacuum spacing, and spin-restricted relaxation can be found in the Supporting Information (Figures S1, S2, and S3, respectively).

Model Amorphous Surfaces. We used model amorphous silica surfaces developed by Ewing et al.[22] to investigate NP−surface interactions. Briefly, the model amorphous silica surface structures were generated as follows: bulk amorphous silica structures were generated using reactive molecular dynamics with the ReaxFF formalism parametrized for silica and water.[23] The structures were then cut into periodic surface slabs, which were hydroxylated by saturating undercoordinated atoms, followed by full relaxation using periodic DFT. Surface structures representing a range of temperatures were generated by simulating the thermodynamics of dehydroxylation using DFT. The temperature corresponding to each particular surface structure was computed based on the energetics of dehydroxylation using a statistical thermodynamics model. For more details, refer to the original published work.[22] These model surfaces have been validated against experimentally measured silanol number and silanol distributions and found to accurately predict silanol number as a function of temperature.[22]

The sizes of the surfaces we used were 23.7 Å × 18.3 Å × ∼12 Å comprising between 250 and 270 atoms. We primarily use the cuboctahedral geometry for Pt_{13}, supplemented by a few calculations using the gas phase global energy minimum structure for Pt_{13}.[24] Experimental characterization of subnan-

DOI: 10.1021/jp5105104
J. Phys. Chem. C 2015, 119, 2503−2512

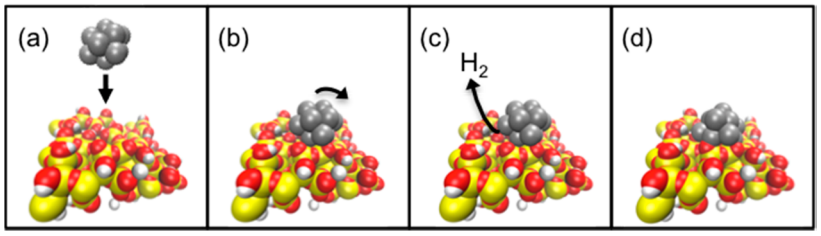

Figure 2. Procedure for simulating NP adsorption. (a) An NP having one of two different orientations is dropped to the surface from 1 of 20 *xy* grid points. Two surfaces are used, each having a different pretreatment temperature, giving a total of 80 different systems. (b) The NP is allowed to rotate using rigid-body approximations and hard-sphere interactions. (c) Pt−O bonds are facilitated by removing H atoms in contact with Pt. (d) The entire system is locally relaxed using DFT.

ometer clusters, such as Pt_{13}, is challenging, and data regarding the atomic structure of Pt_{13} are hence scarce in the literature. However, a number of experimental studies of Pt_{55} (the next larger magic number cluster) supported on amorphous silica surfaces report a cuboctahedral structure,[25−29] motivating the use of this structure in theoretical studies.[9,10,30] Moreover, there are reports of the existence of cuboactahedral Pt_{13} clusters.[31] We hence chose to base most of our calculations on a cuboctahedral structure due to experimental evidence as well as a planned future extension of the present study on the size dependence of catalyst−support interactions, for which the cuboctahedral structure is particularly suitable because it exhibits surfaces that are representative of multiple relevant crystal facets, (100) and (111), as well as steps and corners. We have verified that key results of the present study hold also for the lowest energy gas phase configuration of the Pt_{13} cluster (see discussion in the results section). Starting from vacuum optimized NP structures, shown in Figure 1b, we simulated the adsorption of NPs onto the silica surface using discrete element method[32] (DEM) simulations followed by DFT calculations.

In contrast to supported NPs on crystalline surfaces, generating initial structures of the NPs on the support is nontrivial when modeling amorphous supports; if the NP is too close to the surface, then initial repulsive forces will cause artificial restructuring; if the NP is not close enough to the surface, no relaxation will occur because of the lack of long-range forces in DFT. Simulating NP adsorption (even in the gas phase) onto a support using DFT (e.g., ab initio molecular dynamics) would be computationally expensive. Hence, the use of DEM to generate reasonable starting NP−surface structures is crucial to our methodology. Similar to classical molecular dynamics, particle trajectories are obtained in DEM simulations via Newton's laws of motion for each particle at discrete time. In their simplest form the forces on particles, described by contact mechanics,[33] include normal, Hertzian, repulsion, and gravitational forces, along with tangential friction. For the purpose of our study, the forces in DEM can be limited to only gravity, hard-sphere interactions, and tangential friction, where rebounding of particles (atoms) is completely avoided by tuning the viscoelasticity of the particles in the simulations. This allows for the generation of reasonable initial structures, using negligible computational effort, which can be followed by full relaxation using DFT.

Generating Initial Structures. We generated starting geometries that sample different initial conditions. We considered two different possible orientations of the NP with respect to the silica surface, one with the (100) facet and one with the (111) facet facing the silica surface; these two facets are shown in Figure 1b. Additionally, we considered two different amorphous silica surfaces corresponding to T_{pre} of 200 and 570 °C, shown in Figure 1a. These surfaces correspond to silanol numbers of 4.4 and 1.6 nm^{-2}, respectively.[21] We divided the surfaces with a 5-by-4 grid, resulting in 20 uniformly distributed adsorption sites. Altogether, this resulted in 80 initial geometries that span a range of different local surface sites, NP orientations, as well as different silica pretreatment temperatures corresponding to different silanol numbers.

Simulating NP Adsorption. We simulated the adsorption of Pt on silica using a procedure, illustrated in Figure 2, that generates physically reasonable structures by relaxing all atom positions with DFT. We automated the procedure using a series of Perl and Python codes that perform the following steps for *each* of the systems initialized in the previous step.

(a) Initialization of the Cluster/Support System. Gas-phase optimized cuboctahedral Pt_{13} was placed on a grid point in the *xy* plane above the silica surface.

(b) Dropping the Cluster onto the Surface. The cluster was then dropped onto the surface, by imposing a gravitational force, using a discrete element code[35] invoking the following approximations: (i) all atoms were treated as hard spheres with radius equal to their respective van der Waals radii; (ii) the cluster and surface were treated as rigid bodies; (iii) the particles (i.e., atoms) dissipated energy quickly enough during collisions to avoid any rebounding. The clusters typically rotated to some degree as a result of gravity and a point of hard-sphere contact between NP and surface. These steps generated configurations with sufficiently close NP−surface distances to facilitate relaxation (local optimization) with DFT to strongly bound physisorption states. Typical relaxation energies for physisorbed clusters were 2−3 eV (i.e., the relaxed structures were 2−3 eV lower in energy than the starting configurations). We also verified that these initial configurations were not so close that the NP−surface interaction was repulsive. We confirmed that the energy of each initial condition was lower than the combined energies of the isolated NP and silica slab, indicating that the DFT relaxed geometries are not a result of an initially repulsive NP−surface interaction. The average NP−surface energy, prior to relaxation with DFT, was −0.9 eV for all physisorbed systems.

(c) Cluster−Silica Bond Formation. Experiments have indicated that noble metal clusters (such as Pd_n) supported on silica form metal−oxygen bonds with the support during preparation of the NP−silica catalyst systems, whereas metal−silicon bonds are only formed at higher than typical calcination temperatures.[18,36,37] Our initial calculations confirmed that Pt−O bond formation is also energetically favorable for Pt/silica. Specifically, we found that H migration from silanol to the Pt cluster accompanied by Pt−O bond formation yields a ∼2.4 eV

DOI: 10.1021/jp5105104
J. Phys. Chem. C 2015, 119, 2503−2512

decrease in system energy per Pt−O bond formed. This can be expected because the process involves breaking one bond (O−H) and forming two new bonds (Pt−O and Pt−H). We do not consider kinetic limitations in this process, which are beyond the scope of this study, but rather we assume that the formation of Pt−O bonds occurs whenever there is close contact between the Pt NP and a silanol group. For these reasons, we incorporated a step in our initial geometry preparation that facilitated Pt−O bond formation by removing hydrogen atoms from surface silanols within range to bond to Pt (see Supporting Information for details). For systems with an even number of Pt−O bonds, we assumed that the hydrogen would desorb in the form of H_2. For systems with an odd number of Pt−O bonds formed, a single hydrogen atom was placed on top of the platinum cluster. This was done to allow for spin-restricted DFT calculations, which significantly reduced computational effort. When surface hydrogens were removed, we repeated DEM calculations in step b to allow for better initial geometries for the formation of NP−surface bonds. During this step, the hard sphere radii for Pt and O atoms involved in potential Pt−O binding were set to the covalent radii.

(d) Relaxation of the Cluster/Silica System. Finally all atoms in each system were locally relaxed using DFT using a conjugate gradient algorithm.

RESULTS AND DISCUSSION

NP−Support Binding Interactions. Platinum NPs can bind to the support surface via physisorption or via covalent Pt−O and Pt−Si bonds. We characterized bonding using the simple distance rules for a ball-and-stick molecular model (see Supporting Information for details). Because of the heterogeneity of the silica surface, there is a wide distribution of the number of covalent bonds between Pt and silica, shown in Figure 3. The number of Pt−silica bonds for a single system

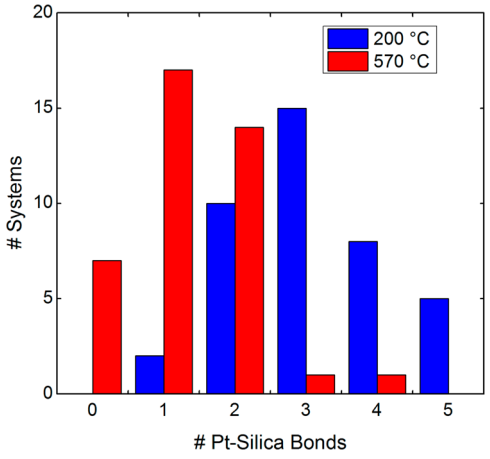

Figure 3. Distribution of the number of Pt−silica bonds (both Pt−O and Pt−Si) for silica surface pretreatment temperatures of 200 and 570 °C, having α_{OH} values of 4.4 and 1.6 nm^2, respectively.

depends on the local silica surface structure at the adsorption site: sites with only siloxane termini typically result in only physisorption, while sites with high silanol density result in multiple Pt−support interfacial bonds. This reflects our assumption that during catalyst preparation O−H bonds are broken but Si−O bonds are not, which is in agreement with experimental observations.[18,37] On average, this approach yields 3.1 and 1.4 covalent Pt−silica bonds for surfaces with T_{pre} = 200 and 570 °C, respectively. In a few cases, we observed Pt−Si bond formation via rupture of a siloxane bridge during relaxation. When visualized, it appears that a Pt atom bonds with both the Si and O atoms involved in a siloxane bridge followed by dissociation of the Si−O bond. Interestingly, the relaxation did not reveal an energy barrier; however, it is unclear whether this is an artifact of the relaxation scheme or not. Interpreting this observation is not within the scope of this study, and these occurrences were rare enough (only 4 cases in 80 systems) that they do not significantly impact the results of this study. Overall, the number of covalent NP−silica bonds formed is inversely related to silica surface pretreatment temperature. This is an expected result because the dehydroxylation of silica results in a lower surface hydroxyl density at higher temperatures. Generally, we expect that the effect of metal−support interactions on the Pt−NP's geometry, electronic properties, and stability will depend on the number of bonds formed between Pt and silica.

Nanoparticle Stability Depends on Support Preparation. Next we consider the impact of silica support properties on nanoparticle stability. Campbell and Sellers have shown that the metal NP chemical potential is fundamental to understanding NP stability because it represents a measure of the thermodynamic driving force for sintering. Rate equations derived from microkinetic models for sintering have shown that the chemical potential of the metal is inversely related to the apparent activation energy of the sintering process, whether the sintering occurs via Ostwald ripening or particle diffusion/coalescence.[3] Furthermore, the chemical potential of a supported metal NP is directly related to its adhesion energy, E_{adh}, defined as the work required to separate the metal/oxide interface in vacuum per interfacial area.[3] Stronger NP adhesion (i.e., more negative E_{adh}) results in lower metal chemical potential. Experiments have indicated that by tailoring the support material, and thus the adhesion energy, NP sintering can be mitigated.[43,44] We calculated the energies associated with distortion of the Pt and silica structures, i.e., deformation energies (see Supporting Information Figure S4), and found that they are small compared to the interaction energies for bonded systems (see Supporting Information Table S1). The adhesion energy times the area of metal−support contact is therefore equivalent to the Pt−silica interaction energy, E_{int}, defined as

$$E_{int} = E_{Pt-S} - E_{Pt}^{fixed} - E_{S-H}^{fixed} \quad (1)$$

where E_{Pt-S} denotes the energy of the NP bound to the silica support, with all atoms relaxed. E_{Pt}^{fixed} and E_{S-H}^{fixed} denote the energies of the NP and support fixed in the relaxed geometries of the Pt−support system. Note that if H atoms were removed from the support surface during the binding procedure, then E_{S-H}^{fixed} involves a surface with dangling bonds.

A linear fit of the data in Figure 4 shows a strong correlation (R^2 = 0.97) between interaction energy and the number of NP−support bonds. The slope of the line is −3.3 eV and gives an estimate of the average bond energy between the NP and the silica surface; these are mainly Pt−O bonds, although a small number (less than 5%) of Pt−Si bonds are also included in this correlation. This value is essentially identical to the bond energy for a Pt−O$^+$ diatomic cation but about 1 eV less attractive than the bond energy of the neutral Pt−O dimer (−4.3 eV).[45] We do not expect that the NP−surface bond energy to be the same as the Pt−O dimer bond energy because

DOI: 10.1021/jp5105104
J. Phys. Chem. C 2015, 119, 2503−2512

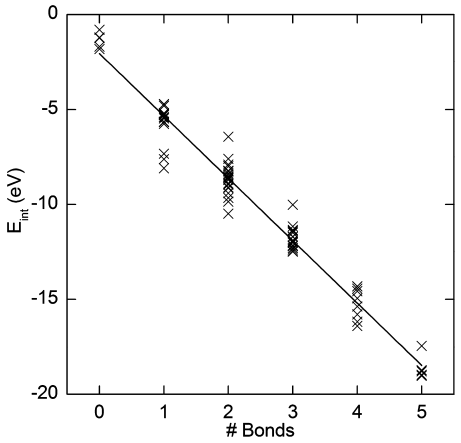

Figure 4. Pt−silica interaction energy as a function of the number of bonds formed between the silica surface and the Pt cluster. The line is a least-squares fit to the data. The coefficient of determination is R^2 = 0.97. The slope, which is an estimate of the energy per bond, is −3.3 eV.

both Pt and O atoms share bonds with other atoms in the NP−silica system. Nevertheless, the fact that the NP−surface bond energy is very similar to the Pt−O dimer bond energy is reassuring. Figure 4 implies that the adhesion energy of supported Pt NPs can be correlated with surface pretreatment temperature because the number of Pt−surface bonds is inversely correlated with T_{pre}. Average interaction energies of −12.4 and −6.8 eV for the T_{pre} = 200 and 570 °C surfaces, respectively, demonstrate the impact pretreatment temperature could have on NP adhesion. These results suggest that support pretreatment temperature may be used to tune catalyst stability; however, further studies will be necessary to elucidate the exact correlation. To determine whether our results are specific to cuboctahedral Pt_{13}, we simulated the adsorption of the theoretical gas phase global minimum Pt_{13} structure[24] using the same procedure that was used for cuboctahedral structures. We used the T_{pre} = 200 °C surface, one orientation, and 20 *xy* gridpoints. We found that the total energies of the supported systems, as functions of the number of Pt−silica bonds (i.e., normalized by the number of atoms in the system), were the same regardless of initial Pt_{13} structure, as shown in Figure S5. The energy of the final structure is thus essentially independent of the energy of the unsupported structure used for the initial conditions. This unexpected result is due to the dominating influence of the interfacial interactions for Pt_{13} NPs.

Metal−Support Interactions Significantly Affect Pt Structure. In this study we aim to gain quantitative insight into Pt−silica interactions by investigating properties that have previously been shown to correlate with catalytic activity. The coordination number (CN) of a metal active site has consistently been shown to correlate strongly with adsorbate binding energy,[6,9,10,46] which can be related to catalytic activity. Figure 5a shows the average distribution of CNs for all 80 supported clusters in this study compared to the unsupported cluster. We calculated both metal−metal coordination (Pt−Pt) and total CN (Pt−*), which includes coordination with Pt, Si, O, and H atoms. We found that the distribution of CNs changed dramatically upon adsorption on the support. The number of accessible low-coordinated sites can be assessed by comparing the Pt−Pt and Pt−* CNs. The number of three- and four-coordinated sites is significantly higher for Pt−Pt than Pt−*. However, there are still many more three and four Pt−* coordinated sites for the supported Pt than unsupported. We therefore conclude that although a significant number of low coordinated sites are inaccessible because they are buried at the interface, a large fraction remains available for binding. We found that the use of the gas phase theoretical global minimum Pt_{13} structue, instead of the cuboctahedral structure, gave almost identical CN distributions for both Pt−Pt and Pt−* (see Figure S6). This comparison shows that our results are not due to the use of a relatively high energy initial Pt cluster structure. Clusters with no Pt−silica bonds had CN distributions more similar to the unsupported cluster (i.e., greater number of five and six coordinated sites) than clusters bonded to the support. However, we did not find clear correlations between structural parameters (such as CNs) and the number of Pt−silica bonds (see Supporting Information Figure S7) except for two general trends: (1) The distribution of CNs becomes broader in systems with Pt−silica bonds. (2) Figure 5b shows that on average, CNs are smaller for supported than for unsupported systems. The reason for the apparent lack of correlation between CN and Pt−silica bonds can be explained by the finding that NP−silica binding has opposite effects on CN of Pt atoms buried at the silica interface and at the exposed NP surface. In the former case, binding to silica

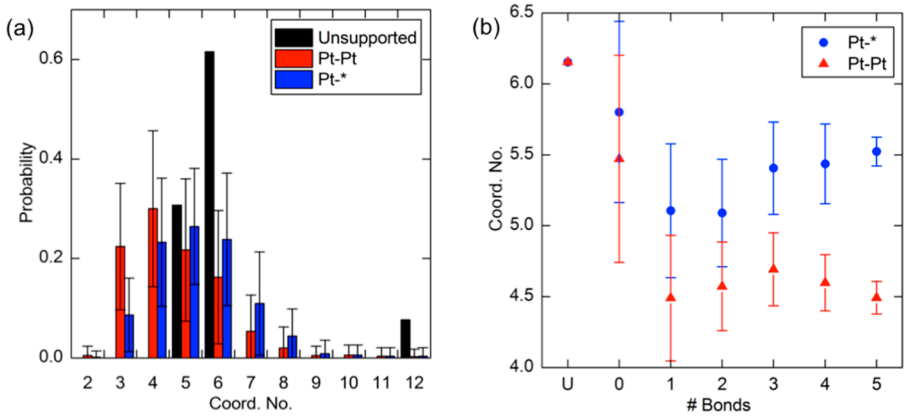

Figure 5. (a) Distribution of atomic coordination numbers for Pt_{13} clusters averaged over all 80 systems in this study: black, unsupported Pt_{13} cluster; red and blue, cluster optimized after placement on silica support (∗ denotes any atom type). (b) Average coordination number vs number of Pt−silica bonds for all 80 systems in this study. U indicates unsupported. Error bars show standard deviation for both (a) and (b).

DOI: 10.1021/jp5105104
J. Phys. Chem. C 2015, 119, 2503−2512

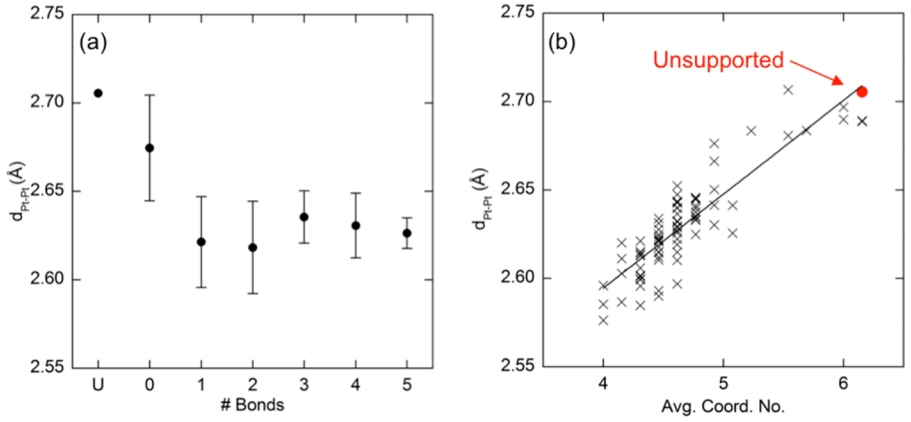

Figure 6. (a) Mean Pt−Pt bond length as a function of number of bonds between Pt and silica, averaged over all 80 systems in this study. U indicates the unsupported NP. Error bars show the standard deviation. (b) Mean Pt−Pt bond length, d_{Pt-Pt}, as a function of the average Pt−Pt coordination number for each of the 80 supported clusters: red circle, unsupported Pt_{13} cluster. The line is a least-squares fit having $R^2 = 0.76$.

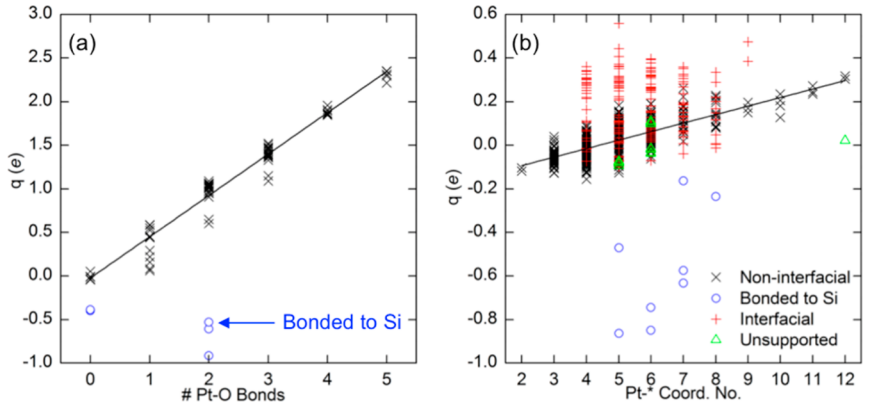

Figure 7. (a) Net charge of Pt cluster (Bader charges) as a function of the number of silica O atoms bonding to the Pt cluster. Data for clusters with one Pt−Si bond are shown as blue circles. The line is a linear fit to the data (excluding systems with Pt−Si bonds). The coefficient of determination is $R^2 = 0.98$. The slope, which is an estimate of the charge transferred per Pt−O bond, is 0.47. (b) Atomic charge on individual Pt atoms as a function of Pt−* coordination number for all Pt atoms in all supported clusters. Red plus signs, blue circles, green triangles, and black × symbols correspond to atoms at the Pt−silica interface, bonded to Si, unsupported cluster, and all other atoms, respectively. The line is a linear fit to the data points represented as × symbols.

leads to an increase of CN (as other Pt atoms are attracted to the Pt/silica interface), and in the latter we observe a decrease of CN (as Pt atoms move away from the exposed surface). In summary, this gives rise to a complicated composite effect.

Metal−metal bond length has been shown to correlate with adsorbate binding strength and could therefore significantly affect catalytic reaction rates.[47] Experiments have shown that subnanometer Pt clusters undergo bond compression when supported on alumina and carbon.[48] Unfortunately, experiments probing metal−metal bonding (e.g., X-ray adsorption near-edge structure or X-ray adsorption fine structure) can only provide average bond lengths and coordination numbers for an entire supported NP at best and hence cannot distinguish between accessible and nonaccessible (e.g., buried in the Pt−silica interface) sites.[48] Figure 6a shows that Pt−silica bonding results in significant Pt−Pt bond compression. This bond compression, furthermore, was consistent between surface, fully coordinated, and interfacial atoms (see Supporting Information Figure S8).

Figure 6b shows that there is an approximately linear relationship between bond compression and average Pt−Pt coordination number. Furthermore, the unsupported Pt_{13} cluster (red dot) lies on the same line as the supported clusters, suggesting that the observed bond compression is essentially a result of reduced (average) CN of the metal NP. This is not unexpected, as surface compression is well-known to occur at solid−gas interfaces. The magnitude of the observed bond compression, however, suggests that the relationship between CN and adsorbate binding energy calculated using surfaces or fixed bulk geometries[6,9,10] may be significantly different than for fully relaxed small supported clusters, in particular, on amorphous supports. On the basis of our results, we expect the effects of metal−support interactions on adsorbate binding energies to be complicated because NP−support interactions give rise to two competing phenomena, namely, an increase in bond compression, which generally weakens adsorbate binding, and a decrease in CN, which generally enhances adsorbate binding.

Electronic Structure Is Affected by Both Reconstruction and Metal−Support Bonds. Localization of electron density around active sites can affect adsorbate binding significantly. Generally, electron acceptors (e.g., O_2) bind preferentially to negatively charged sites while positive charge strengthens binding of electron donors (e.g., CO).[49] We calculated Bader charges for all optimized NPs with and without the support. Figure 7a shows that physisorbed clusters

DOI: 10.1021/jp5105104
J. Phys. Chem. C 2015, 119, 2503−2512

have a net charge close to zero and clusters become increasingly cationic with the number of Pt−O bonds. Charge transfer from the cluster to support is linearly dependent on the number of Pt−O bonds, reaching over 2*e* for clusters with five Pt−O bonds. This magnitude of charge transfer has been shown to dramatically impact catalytic reactions.[50] We therefore expect that this charge transfer may significantly impact adsorbate binding and hence catalytic activity. Pt−Si bonding results in significant charge transfer from the silica surface into the Pt_{13} (blue points in Figure 7a). The magnitude of charge transfer is considerable for Pt−Si and Pt−O bonds, resulting in individual Pt atomic charges of (up to −1.0*e* and +0.6*e*, respectively). Figure 7b shows that in general, for noninterfacial atoms, atomic charge is more positive with increasing CN. Pt atoms at the Pt−silica interface can have a significant positive charge and many of these have relatively small Pt−* CN, indicating that they are accessible to adsorbates, as illustrated in Figure 8. This

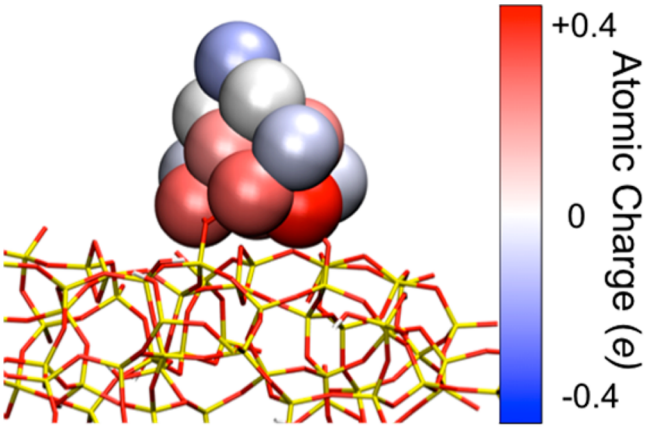

Figure 8. Distribution of charges on a supported Pt_{13} cluster with two Pt−O bonds. Atoms bonding to hydroxyls and their neighbors clearly undergo charge depletion, whereas low coordinated atoms not near the silica surface have slightly negative charges.

suggests that electron donor molecules may preferentially bind at the perimeter of the Pt−silica interface. The linear relation between nanoparticle charge and both number of Pt−silica bonds and coordination number, respectively, has important consequences for experimental probes of CNs or NP−silica bonds. For example, the IR frequency of the CO stretch is known to be sensitive to surface charge[51] and could be used to experimentally probe for CNs and number of NP−silica bonds via the correlation observed in Figure 7b.

Although Pt_{13} is small enough that the d density of states (DOS) is discretized,[9] the d-band center (average energy of the d states) has been shown to correlate with adsorbate binding energies for 12 and 13 atom clusters.[6,10] In general, adsorbate−metal bonding for transition metals results in bonding and antibonding states. Lower d-band center corresponds to increased filling of the antibonding states upon adsorbate binding and hence to weaker binding strength.[52,53] We have calculated the density of states for each individual Pt atom, from which we calculated the d-band center, d_c, as

$$d_c = \frac{\sum e_i \rho_i}{\sum \rho_i} \tag{2}$$

where e_i is the eigenvalue of state i and ρ_i is the density of state i. We considered states with eigenvalues between −8 and +6 eV. In agreement with previous studies,[6,10] we found that the d-band center for Pt atoms roughly correlates with CN, when considering all atoms in the isolated cluster. When analyzing Pt atoms for all supported Pt_{13} systems in this study, however, there is at best a weak correlation between d-band center and CN (see Supporting Information Figure S9). To test if this lack of correlation is due to the wide range of geometries observed in this study, we analyzed each system individually. We fit the d-band center as a function of the CN for each individual system with a linear equation and calculated the coefficient of determination (R^2). We found that for almost all systems there was no clear correlation between the d-band center and the Pt−Pt CN. The results clearly indicate that it is not just the wide range of different geometries on amorphous supports but that CN cannot be used to predict relative d-band centers for adsorption sites on silica-supported Pt_{13}, even when considering a single supported cluster (see Supporting Information Figure S10).

Recent work has shown that it is more appropriate to treat small, supported metal clusters as molecules rather than small pieces of bulk metal.[4,11] We therefore considered the d-bands of entire Pt clusters. Supporting Pt_{13} on silica did not result in a consistent perturbation of the d-DOS; however, d-band centers for supported systems varied significantly from about −1.87 to −1.64 eV, compared to −1.75 eV for the unsupported cluster (see Supporting Information Figure S11). When recalculating the DOS for systems after removing the support (but fixing the reconstructed Pt geometry), we found that the d-DOS is unaffected by Pt−silica bonds. This means that the wide range of d-band centers observed is due to the degree of reconstruction caused by metal−support interactions upon adsorption of the NP and not electronic interactions with the support.

Supporting the notion that small supported metal clusters behave as molecules, previous theoretical investigations have shown that, for small metal clusters, the frontier orbitals (the highest occupied molecular oribital (HOMO) and lowest unoccupied molecular orbital (LUMO)) can be used to accurately predict relative binding energies of adsorbates.[4] In particular, binding properties of electron acceptors and donors are particularly well correlated with the localization of the HOMO and LUMO, respectively, on small metal clusters.[4,54] We therefore performed a qualitative analysis on a number of the systems in this study to investigate the effects of Pt−silica interactions on frontier orbitals. We found that supporting the cluster on amorphous silica can have a dramatic impact on the "extent" (i.e., the size of an atomic orbital at constant isovalue) and directionality of both the HOMO and LUMO at different surface sites. These effects could be a result of multiple factors: (1) significant distortion of the cluster geometry, (2) Pt−O bond formation, and (3) noncovalent (van der Waals and electrostatic) interactions between cluster and support. To isolate the effects of these factors, Figure 9 shows a comparison of the HOMO and LUMO for Pt_{13} relaxed in vacuum (unsupported), relaxed on the silica surface, and relaxed on the silica surface followed by the removal of the silica support. This allowed us to discern the roles of geometric reconstruction (unsupported vs supported) and Pt−silica interactions (supported, with vs without silica atoms).

We discovered a number of general trends for all observed systems. First, it is clear by comparing the first two columns of Figure 9 that distortion of the cluster geometry due to NP−support interactions results in dramatic changes to both the

DOI: 10.1021/jp5105104
J. Phys. Chem. C 2015, 119, 2503−2512

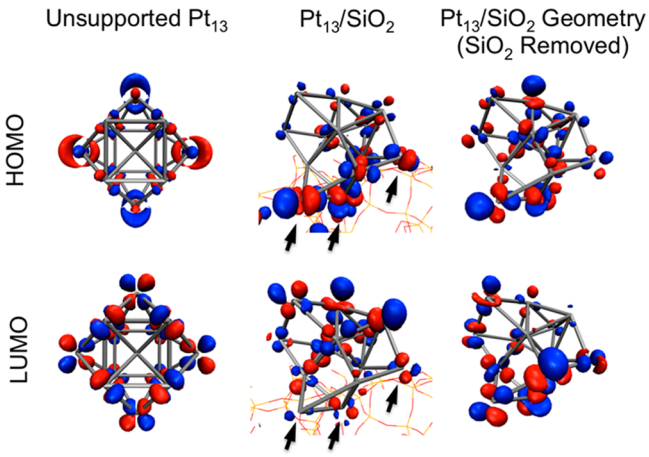

Figure 9. Representative images of the HOMO and LUMO for unsupported cuboctahedral Pt_{13}, Pt_{13}/SiO_2, and Pt_{13}/SiO_2 with silica atoms removed. Arrows indicate Pt−O bonds.

extent and directionality of the HOMO and LUMO. Comparison of the supported Pt cluster with and without silica atoms (second and third columns of Figure 9) demonstrates the effects of Pt−O bond formation on the frontier orbitals. In general, we found that Pt−O bonds significantly affect the extent of the HOMO and LUMO in a consistent way. Near Pt−O bonds, the extent of the HOMO is increased while the LUMO is reduced. For atoms far from Pt−O bonds, however, the extent of the LUMO is increased while the HOMO is reduced. This can be interpreted as the formation of Pt−O bonds "pulling" the HOMO in while "pushing" the LUMO away. Analyses of supported Pt_{13} systems with no Pt−O bond formation show that noncovalent Pt−silica interactions have negligible effects on the frontier orbitals (see Supporting Information Tables S2 and S3).

The effect of NP−silica binding on the frontier orbitals is expected to influence adsorbate binding in the opposite way to charge distribution, discussed above. In particular, the increase of the HOMO amplitude near Pt−O bonds suggests that the affinity to bind electron acceptors (e.g., O_2) at the Pt−silica interface is increased upon forming Pt−silica bonds. Conversely, the reduction of LUMO amplitude near Pt−O bonds suggests that the binding affinity for electron donors (e.g., CO) at the Pt−silica interface will be decreased. NP−silica binding thus results in competing phenomena: redistribution of the frontier orbitals and electron density distribution. As we have already seen for the geometric parameters, the correlation between structure (deformation) and NP−silica binding is quite complicated because of a superposition of multiple effects. It can therefore be expected that the impact of NP−support binding on catalyst−substrate adsorption may also be quite convoluted. A detailed study of NP−substrate binding thus requires significant development that goes beyond the scope of this work and will be presented in a future publication.

CONCLUSIONS

We have developed a methodology for studying metal nanoparticles on amorphous supports, which can be applied to a number of NP and support materials. Our approach uses a combination of the discrete element method and DFT calculations to generate model systems of supported NPs. We used this method to quantitatively investigate the impact of an amorphous silica surface on the morphology, electronic structure, and energetics of supported Pt_{13} clusters. Our results reveal that the support significantly alters the physicochemical properties of the adsorbed NP. A summary of our findings is as follows:

1. Our results suggest that surface pretreatment temperature can be used to tune the Pt−SiO_2 interface and thus stability of silica-supported nanoparticles because the number of Pt−silica bonds is a function of the pretreatment temperature. Experiments to validate this prediction are currently underway.
2. Charge transfer from Pt to silica, via Pt−O bonds, is strongly correlated with the silica silanol number and results in charge depletion of Pt atoms near the perimeter of the NP−silica interface.
3. Adsorption of Pt_{13} NP clusters on amorphous silica results in considerable relaxation of the NP. The surface-mediated relaxation leads to substantial lowering of average Pt coordination numbers and significant Pt−Pt bond compression and dramatically affects the d-band centers and frontier orbitals.
4. The frontier orbitals are significantly affected by both the distortion of the Pt NP cluster due to adsorption and electronic effects from the silica support. The effects of NP−silica binding on the frontier orbitals and charge distribution result in competing influence on adsorbate binding behavior.

The extent of the impact of support interactions with Pt_{13} NPs, i.e., the strong effect of the Pt−SiO_2 interface, means that experimental attempts to measure the innate properties of very small NP catalysts will likely fail because the measurable physical and chemical properties will depend critically on NP−support interactions, which will vary significantly across the surface of an amorphous support. Furthermore, the magnitude and complexity of the changes to NP properties induced by catalyst−support interactions indicate that the adsorbate binding properties of these systems cannot be accurately predicted by studying either the corresponding freestanding clusters or Pt_{13} on perfectly crystalline silica surfaces; i.e., the accurate description of the Pt−SiO_2 interface is critical. The range of effects observed in this study further indicates that single geometric and electronic descriptors for adsorbate binding may not hold much meaning for subnanometer clusters on amorphous supports. Many trends determined for larger or freestanding clusters, therefore, cannot be expected to extrapolate to very small (i.e., 13 atom and smaller) metal clusters on amorphous supports. In future work we will thus investigate the impact of metal−support interactions on NP properties as a function of cluster size.

ASSOCIATED CONTENT

Supporting Information

Procedure details, validation of model parameters, deformation energies, coordination numbers as a function of number of bonds, detailed metal−metal bond compression data, d-band center plots, and additional HOMO/LUMO plots with density difference plots. This material is available free of charge via the Internet at http://pubs.acs.org.

AUTHOR INFORMATION

Corresponding Author

*E-mail: qclab@pitt.edu.

DOI: 10.1021/jp5105104
J. Phys. Chem. C 2015, 119, 2503−2512

Notes

The authors declare no competing financial interest.

■ ACKNOWLEDGMENTS

This work was supported by the Department of Education GAANN program (Grant P200A100087) and the Mascaro Center for Sustainable Innovation at the University of Pittsburgh. This work used the Extreme Science and Engineering Discovery Environment (XSEDE), Grant TG-CHE140046, which is supported by National Science Foundation Grant ACI-1053575. D.S.L. acknowledges financial support by the Central Research Development Fund (CRDF) at the University of Pittsburgh. Computational resources at the University of Pittsburgh's Center for Simulation and Modeling are also acknowledged. S.J.P. acknowledges support from an Arts & Sciences Undergraduate Research award from the University of Pittsburgh.

■ REFERENCES

(1) An, N. H.; Zhang, W. L.; Yuan, X. L.; Pan, B.; Liu, G.; Jia, M. J.; Yan, W. F.; Zhang, W. X. Catalytic oxidation of formaldehyde over different silica supported platinum catalysts. *Chem. Eng. J.* **2013**, *215*, 1−6.

(2) Campbell, C. T.; Parker, S. C.; Starr, D. E. The effect of size-dependent nanoparticle energetics on catalyst sintering. *Science* **2002**, *298*, 811−814.

(3) Campbell, C. T.; Sellers, J. R. V. Anchored metal nanoparticles: Effects of support and size on their energy, sintering resistance and reactivity. *Faraday Discuss.* **2013**, *162*, 9−30.

(4) Chretien, S.; Buratto, S. K.; Metiu, H. Catalysis by very small Au clusters. *Curr. Opin. Solid State Mater. Sci.* **2007**, *11*, 62−75.

(5) Jiang, C. X.; Hara, K.; Fukuoka, A. Low-Temperature Oxidation of Ethylene over Platinum Nanoparticles Supported on Mesoporous Silica. *Angew. Chem., Int. Ed.* **2013**, *52*, 6265−6268.

(6) Jiang, T.; Mowbray, D. J.; Dobrin, S.; Falsig, H.; Hvolbaek, B.; Bligaard, T.; Norskov, J. K. Trends in CO Oxidation Rates for Metal Nanoparticles and Close-Packed, Stepped, and Kinked Surfaces. *J. Phys. Chem. C* **2009**, *113*, 10548−10553.

(7) Kim, M.-Y.; Jung, S. B.; Kim, M. G.; You, Y. S.; Park, J.-H.; Shin, C.-H.; Seo, G. Preparation of Highly Dispersive and Stable Platinum Catalysts Supported on Siliceous SBA-15 Mesoporous Material: Roles of Titania Layer Incorporation and Hydrogen Peroxide Treatment. *Catal. Lett.* **2009**, *129*, 194−206.

(8) Kim, M.-Y.; Park, J.-H.; Shin, C.-H.; Han, S.-W.; Seo, G. Dispersion Improvement of Platinum Catalysts Supported on Silica, Silica-Alumina and Alumina by Titania Incorporation and pH Adjustment. *Catal. Lett.* **2009**, *133*, 288−297.

(9) Li, L.; Larsen, A. H.; Romero, N. A.; Morozov, V. A.; Glinsvad, C.; Abild-Pedersen, F.; Greeley, J.; Jacobsen, K. W.; Norskov, J. K. Investigation of Catalytic Finite-Size-Effects of Platinum Metal Clusters. *J. Phys. Chem. Lett.* **2013**, *4*, 222−226.

(10) Peterson, A. A.; Grabow, L. C.; Brennan, T. P.; Shong, B. G.; Ooi, C. C.; Wu, D. M.; Li, C. W.; Kushwaha, A.; Medford, A. J.; Mbuga, F.; Li, L.; Norskov, J. K. Finite-Size Effects in O and CO Adsorption for the Late Transition Metals. *Top. Catal.* **2012**, *55*, 1276−1282.

(11) Mpourmpakis, G.; Vlachos, D. G. The Effects of the MgO Support and Alkali Doping on the CO Interaction with Au. *J. Phys. Chem. C* **2009**, *113*, 7329−7335.

(12) Kim, M. Y.; Park, S. M.; Park, J. H.; Shin, C. H.; Moon, W. J.; Sung, N. E.; Seo, G. Platinum catalysts supported on silicas: effect of silica characteristics on their catalytic activity in carbon monoxide oxidation. *React. Kinet., Mech. Catal.* **2011**, *103*, 463−479.

(13) Norskov, J. K.; Bligaard, T.; Rossmeisl, J.; Christensen, C. H. Towards the computational design of solid catalysts. *Nat. Chem.* **2009**, *1*, 37−46.

(14) Hu, C. H.; Chizallet, C.; Mager-Maury, C.; Corral-Valero, M.; Sautet, P.; Toulhoat, H.; Raybaud, P. Modulation of catalyst particle structure upon support hydroxylation: Ab initio insights into Pd-13 and Pt-13/gamma-Al_2O_3. *J. Catal.* **2010**, *274*, 99−110.

(15) Kim, H. Y.; Henkelman, G. CO Oxidation at the Interface between Doped CeO_2 and Supported Au Nanoclusters. *J. Phys. Chem. Lett.* **2012**, *3*, 2194−2199.

(16) Kim, H. Y.; Lee, H. M.; Henkelman, G. CO Oxidation Mechanism on CeO_2-Supported Au Nanoparticles. *J. Am. Chem. Soc.* **2012**, *134*, 1560−1570.

(17) Eswaramoorthy, M.; Niwa, S.; Toba, M.; Shimada, H.; Raj, A.; Mizukami, F. The conversion of methane with silica-supported platinum catalysts: the effect of catalyst preparation method and platinum particle size. *Catal. Lett.* **2001**, *71*, 55−61.

(18) Min, B. K.; Santra, A. K.; Goodman, D. W. Understanding silica-supported metal catalysts: Pd/silica as a case study. *Catal. Today* **2003**, *85*, 113−124.

(19) Huang, S. J.; Hara, K.; Fukuoka, A. Intrinsic Catalytic Role of Mesoporous Silica in Preferential Oxidation of Carbon Monoxide in Excess Hydrogen. *Chemistry—Eur. J.* **2012**, *18*, 4738−4747.

(20) Cargnello, M.; Doan-Nguyen, V. V. T.; Gordon, T. R.; Diaz, R. E.; Stach, E. A.; Gorte, R. J.; Fornasiero, P.; Murray, C. B. Control of Metal Nanocrystal Size Reveals Metal-Support Interface Role for Ceria Catalysts. *Science* **2013**, *341*, 771−773.

(21) Zhuravlev, L. T. The surface chemistry of amorphous silica. Zhuravlev model. *Colloids Surf., A* **2000**, *173*, 1−38.

(22) Ewing, C. S.; Bhavsar, S.; Veser, G.; McCarthy, J. J.; Johnson, J. K. Accurate Amorphous Silica Surface Models from First-Principles Thermodynamics of Surface Dehydroxylation. *Langmuir* **2014**, *30*, 5133−5141.

(23) Fogarty, J. C.; Aktulga, H. M.; Grama, A. Y.; van Duin, A. C. T.; Pandit, S. A. A reactive molecular dynamics simulation of the silica-water interface. *J. Chem. Phys.* **2010**, *132*, 174704.

(24) Chou, J. P.; Hsing, C. R.; Wei, C. M.; Cheng, C.; Chang, C. M. Ab initio random structure search for 13-atom clusters of fcc elements. *J. Phys.: Condens. Matter* **2013**, *25*, 125305.

(25) Cuenya, B. R.; Croy, J. R.; Mostafa, S.; Behafarid, F.; Li, L.; Zhang, Z. F.; Yang, J. C.; Wang, Q.; Frenkel, A. I. Solving the Structure of Size-Selected Pt Nanocatalysts Synthesized by Inverse Micelle Encapsulation. *J. Am. Chem. Soc.* **2010**, *132*, 8747−8756.

(26) Cuenya, B. R.; Frenkel, A. I.; Mostafa, S.; Behafarid, F.; Croy, J. R.; Ono, L. K.; Wang, Q. Anomalous lattice dynamics and thermal properties of supported size- and shape-selected Pt nanoparticles. *Phys. Rev. B* **2010**, *82*, 155450.

(27) Cuenya, B. R.; Ortigoza, M. A.; Ono, L. K.; Behafarid, F.; Mostafa, S.; Croy, J. R.; Paredis, K.; Shafai, G.; Rahman, T. S.; Li, L.; Zhang, Z.; Yang, J. C. Thermodynamic properties of Pt nanoparticles: Size, shape, support, and adsorbate effects. *Phys. Rev. B* **2011**, *84*, 245438.

(28) Li, L.; Wang, L. L.; Johnson, D. D.; Zhang, Z. F.; Sanchez, S. I.; Kang, J. H.; Nuzzo, R. G.; Wang, Q.; Frenkel, A. I.; Li, J.; Ciston, J.; Stach, E. A.; Yang, J. C. Noncrystalline-to-Crystalline Transformations in Pt Nanoparticles. *J. Am. Chem. Soc.* **2013**, *135*, 13062−13072.

(29) Mostafa, S.; Behafarid, F.; Croy, J. R.; Ono, L. K.; Li, L.; Yang, J. C.; Frenkel, A. I.; Cuenya, B. R. Shape-Dependent Catalytic Properties of Pt Nanoparticles. *J. Am. Chem. Soc.* **2010**, *132*, 15714−15719.

(30) Xu, D.; Liu, Y. J.; Zhao, J. X.; Cai, Q. H.; Wang, X. Z. Theoretical Study of the Deposition of Pt Clusters on Defective Hexagonal Boron Nitride (h-BN) Sheets: Morphologies, Electronic Structures, and Interactions with O. *J. Phys. Chem. C* **2014**, *118*, 8868−8876.

(31) Bartolome, J.; Bartolome, F.; Garcia, L. M.; Roduner, E.; Akdogan, Y.; Wilhelm, F.; Rogalev, A. Magnetization of Pt-13 clusters supported in a NaY zeolite: A XANES and XMCD study. *Phys. Rev. B* **2009**, *80*, 10.

(32) Cundall, P. A.; Strack, O. D. L. Discrete Numerical-Model for Granular Assemblies. *Geotechnique* **1979**, *29*, 47−65.

(33) Johnson, K. L. *Contact Mechanics*; Cambridge University Press: Cambridge, U.K., 1987.

DOI: 10.1021/jp5105104
J. Phys. Chem. C 2015, 119, 2503−2512

(34) Humphrey, W.; Dalke, A.; Schulten, K. VMD: Visual molecular dynamics. *J. Mol. Graphics Model.* **1996**, *14*, 33−38.
(35) McCarthy, J. J.; Ottino, J. M. Particle dynamics simulation: a hybrid technique applied to granular mixing. *Powder Technol.* **1998**, *97*, 91−99.
(36) Moroz, E. M.; Kriventsov, V. V.; Kochubei, D. I. EuroPt-1 catalyst: Radial distribution of electron density X-ray diffraction and EXAFS studies. *J. Struct. Chem.* **2009**, *50*, 1082−1087.
(37) Schwartz, J. M.; Schmidt, L. D. Microstructures of Pt-Ce and Rh-Ce Particles on Alumina and Silica. *J. Catal.* **1992**, *138*, 283−293.
(38) VandeVondele, J.; Krack, M.; Mohamed, F.; Parrinello, M.; Chassaing, T.; Hutter, J. QUICKSTEP: Fast and accurate density functional calculations using a mixed Gaussian and plane waves approach. *Comput. Phys. Commun.* **2005**, *167*, 103−128.
(39) Hammer, B.; Hansen, L. B.; Norskov, J. K. Improved adsorption energetics within density-functional theory using revised Perdew−Burke−Ernzerhof functionals. *Phys. Rev. B* **1999**, *59*, 7413−7421.
(40) Goedecker, S.; Teter, M.; Hutter, J. Separable dual-space Gaussian pseudopotentials. *Phys. Rev. B* **1996**, *54*, 1703−1710.
(41) Krack, M. Pseudopotentials for H to Kr optimized for gradient-corrected exchange-correlation functionals. *Theor. Chem. Acc.* **2005**, *114*, 145−152.
(42) VandeVondele, J.; Hutter, J. Gaussian basis sets for accurate calculations on molecular systems in gas and condensed phases. *J. Chem. Phys.* **2007**, *127*, 114105.
(43) Kalakkad, D.; Datye, A. K.; Robota, H. Interaction of Platinum and Ceria Probed by Transmission Electron-Microscopy and Catalytic Reactivity. *Appl. Catal., B* **1992**, *1*, 191−219.
(44) Libuda, J.; Frank, M.; Sandell, A.; Andersson, S.; Bruhwiler, P. A.; Baumer, M.; Martensson, N.; Freund, H. J. Interaction of rhodium with hydroxylated alumina model substrates. *Surf. Sci.* **1997**, *384*, 106−119.
(45) Luo, Y. R. *Comprehensive Handbook of Chemical Bond Energies*; CRC Press: Boca Raton, FL, 2007.
(46) Kleis, J.; Greeley, J.; Romero, N. A.; Morozov, V. A.; Falsig, H.; Larsen, A. H.; Lu, J.; Mortensen, J. J.; Dulak, M.; Thygesen, K. S.; Norskov, J. K.; Jacobsen, K. W. Finite Size Effects in Chemical Bonding: From Small Clusters to Solids. *Catal. Lett.* **2011**, *141*, 1067−1071.
(47) Mavrikakis, M.; Hammer, B.; Norskov, J. K. Effect of strain on the reactivity of metal surfaces. *Phys. Rev. Lett.* **1998**, *81*, 2819−2822.
(48) Frenkel, A. I.; Small, M. W.; Smith, J. G.; Nuzzo, R. G.; Kvashnina, K. O.; Tromp, M. An in Situ Study of Bond Strains in 1 nm Pt Catalysts and Their Sensitivities to Cluster−Support and Cluster−Adsorbate Interactions. *J. Phys. Chem. C* **2013**, *117*, 23286−23294.
(49) Wallace, W. T.; Whetten, R. L. Carbon monoxide adsorption on selected gold clusters: Highly size-dependent activity and saturation compositions. *J. Phys. Chem. B* **2000**, *104*, 10964−10968.
(50) Stamatakis, M.; Christiansen, M. A.; Vlachos, D. G.; Mpourmpakis, G. Multiscale Modeling Reveals Poisoning Mechanisms of MgO-Supported Au Clusters in CO Oxidation. *Nano Lett.* **2012**, *12*, 3621−3626.
(51) Rodriguez, J. A.; Truong, C. M.; Goodman, D. W. Infrared Vibrational Studies of CO Adsorption on Cu/Pt(111) and CuPt(111) Surfaces. *J. Chem. Phys.* **1992**, *96*, 7814−7825.
(52) Hammer, B.; Norskov, J. K. Electronic factors determining the reactivity of metal surfaces. *Surf. Sci.* **1995**, *343*, 211−220.
(53) Nilsson, A.; Pettersson, L. G. M.; Hammer, B.; Bligaard, T.; Christensen, C. H.; Norskov, J. K. The electronic structure effect in heterogeneous catalysis. *Catal. Lett.* **2005**, *100*, 111−114.
(54) Mpourmpakis, G.; Andriotis, A. N.; Vlachos, D. G. Identification of Descriptors for the CO Interaction with Metal Nanoparticles. *Nano Lett.* **2010**, *10*, 1041−1045.

DOI: 10.1021/jp5105104
J. Phys. Chem. C 2015, 119, 2503−2512